CHIRALITY 20:796–804 (2008)

Stereoselective Disposition of *S*- and *R*-Licarbazepine in Mice

GILBERTO ALVES,[1] ISABEL FIGUEIREDO,[1] AMÍLCAR FALCÃO,[1]* MARGARIDA CASTEL-BRANCO,[1] MARGARIDA CARAMONA,[1] AND PATRÍCIO SOARES-DA-SILVA[2]

[1]*Faculty of Pharmacy, Laboratory of Pharmacology, Coimbra University, Coimbra, Portugal*
[2]*Department of Research and Development, BIAL, S. Mamede do Coronado, Portugal*

ABSTRACT The stereoselective disposition of *S*-licarbazepine (*S*-Lic) and *R*-licarbazepine (*R*-Lic) was investigated in plasma, brain, liver, and kidney tissues after their individual administration (350 mg/kg) to mice by oral gavage. Plasma, brain, liver, and kidney concentrations of licarbazepine enantiomers and their metabolites were determined over the time by a validated chiral HPLC-UV method. The mean concentration data, attained at each time point, were analyzed using a non-compartmental model. *S*-Lic and *R*-Lic were rapidly absorbed from gastrointestinal tract of mouse and immediately distributed to tissues supplied with high blood flow rates. Both licarbazepine enantiomers were metabolized to a small extent, each parent compound being mainly responsible for the systemic and tissue drug exposure. The stereoselectivity in the metabolism and distribution of *S*- and *R*-Lic was easily identified. An additional metabolite was detected following *R*-Lic administration and *S*-Lic showed a particular predisposition for hepatic and renal accumulation. Stereoselective processes were also identified at the blood–brain barrier, with the brain exposure to *S*-Lic almost twice that of *R*-Lic. Another finding, reported here for the first time, was the ability of the mouse to perform the chiral inversion of *S*- and *R*-Lic, albeit to a small extent. *Chirality 20:796–804, 2008.*

KEY WORDS: stereoselectivity; licarbazepine enantiomers; eslicarbazepine acetate; oxcarbazepine; pharmacokinetics; chiral separation; mouse plasma and tissues

It is widely known that enantiomers of chiral drugs may have different pharmacodynamic, pharmacokinetic and toxicological effects upon biological systems.[1,2] Differences in the biological activity may be intrinsically related to the pharmacodynamics of each enantiomer or may be due to differences in their pharmacokinetics, with different blood or tissue concentration-time profiles. It is generally accepted that the drug metabolism introduces the greatest degree of chiral discrimination in pharmacokinetic processes, although other mechanisms in the body, among which the absorption, protein and tissue binding, distribution and excretion, may also contribute to the stereoselective drug disposition.[3–6] Hence, chirality has emerged as a critical issue in drug design, since the regulatory agencies now require pharmacological and toxicological studies not only on the racemate but also on both enantiomers before granting approval of a new chiral drug.[2]

Eslicarbazepine acetate (ESL), or *S*-licarbazepine acetate, previously known as BIA 2-093, is a new chiral drug currently undergoing clinical development for the treatment of epilepsy.[7] The molecule of licarbazepine acetate contains a chiral center at the tenth position, where an asymmetric carbon atom is attached to four different ligands, and accordingly exists as two enantiomers, ESL and its antipode *R*-licarbazepine acetate (BIA 2-059).[8,9] ESL, *R*-licarbazepine acetate and their racemic mixture, as well as other related compounds, were orally assessed in rats for anticonvulsant activity and compared with carbamazepine (CBZ) and oxcarbazepine (OXC). Surprisingly, the licarbazepine acetate enantiomers showed to possess strikingly different anticonvulsant properties. ESL was clearly the most potent with anticonvulsant potency similar to CBZ and higher than OXC, while *R*-licarbazepine acetate was almost devoid of activity and the racemic mixture demonstrated an intermediate potency.[8] These findings suggest that such differences could be due to the stereochemistry at the carbon-10 chiral center by itself or attributed to differences in their absorption, distribution, metabolism or excretion processes. Therefore, Hainzl et al.[9] performed some in vitro and in vivo experimental studies with ESL and its R-enantiomer in order to get enough pharmacokinetic data to understand their distinct pharmacodynamic properties. Subsequently, it was found that ESL and its stereoisomer *R*-licarbazepine acetate were rapidly hydrolyzed to their corresponding hydroxy deriva-

Contract grant sponsor: Foundation for Science and Technology, Portugal; Contract grant number: SFRH/BD/12694/2003; Contract grant sponsor: BIAL, Portugal.
*Correspondence to: Amílcar Falcão, Ph.D., Faculty of Pharmacy, Laboratory of Pharmacology, Coimbra University, 3000-141 Coimbra, Portugal. E-mail: acfalcao@ff.uc.pt
Received for publication 19 November 2007; Accepted 10 January 2008
DOI: 10.1002/chir.20546
Published online 27 February 2008 in Wiley InterScience (www.interscience.wiley.com).

tives, *S*-licarbazepine (*S*-Lic) and *R*-licarbazepine (*R*-Lic), respectively. However, *R*-Lic undergoes a further oxidation to the *trans*-diol metabolite, demonstrating an increased predisposition to earlier inactivation. Indeed, the *trans*-diol is an inactive metabolite also produced from the metabolism of CBZ and OXC.[10]

Thus, ESL is being developed as a third generation to CBZ or a second generation to OXC,[11] but it is more closely related to OXC from a metabolic point of view. Briefly, OXC is an achiral prodrug which, in humans, is rapidly reduced in liver to the pharmacologically active metabolite licarbazepine or 10-hydroxy-carbazepine.[12] Nevertheless, OXC first-pass reduction to licarbazepine is stereoselective, appearing in plasma as *S*-Lic and *R*-Lic in approximately a 4:1 enantiomeric ratio.[13–15] Concerning to the metabolism of ESL, it is not yet well established if its deacetylation occurs in the gastrointestinal tract, in blood instantly after absorption or in liver.[9,16] In contrast, it is well known that in humans ESL is quickly and extensively metabolized to *S*-Lic (>95%) and, to a minor extent, to *R*-Lic and OXC.[17–19] Thereby, *S*-Lic is the most relevant metabolite of ESL and OXC, exemplifying chirality preservation and stereoselective metabolism, respectively. However, since low concentrations of *R*-Lic are also produced from ESL, the absolute enantioselectivity in the metabolism of ESL was not observed.

To date, in spite of OXC being used in clinical practice for several years and ESL being in its final phase of clinical trials, few studies explored the differential pharmacokinetics of licarbazepine enantiomers or the bi-directional chiral inversion.[9,20] As a result, taking into account the species-dependent metabolism of OXC and ESL, in this case among small laboratory animals, the mouse seems to be the most relevant species to humans from a metabolic point of view.[9,17,18,19] The current study was firstly designed to investigate the disposition and chiral inversion of *S*-Lic and *R*-Lic, and secondly, to examine the stereoselectivity in the pharmacokinetics of both enantiomers after their separate administration to mice by oral gavage.

MATERIALS AND METHODS

Chemicals

S-Lic (BIA 2-194, lot number PC020131B, 99.79% pure by HPLC), *R*-Lic (BIA 2-195, lot number PC040414, 100% pure by HPLC), OXC (lot number 97.12.17, >98% pure by HPLC) and BIA 2-265 (lot number PC050704, 97.4% pure by HPLC) used as internal standard (IS), were synthesized by BIAL (Porto, Portugal) (see Fig. 1). Methanol (HPLC grade, SDS), water milli-Q (HPLC grade, >15 MΩ, homemade), acetonitrile, ethyl acetate, sodium dihydrogen phosphate dihydrate, di-sodium hydrogen phosphate dehydrate and hydrochloric acid 37% were purchased from Merck KGaA (Darmstadt, Germany). Carboxymethylcellulose sodium salt for drug suspension was obtained from Sigma (St. Louis, USA).

Animals and Experimental Design

Adult male CD-1 mice obtained from Harlan-Interfauna (Barcelona, Spain) weighing 30–35 g were used. The animals were housed in local animal facilities, in a light (12 h light/dark cycle) and temperature (22°C ± 1°C) controlled environment, for at least 5 days prior to the experiments. A regular chow diet (4RF21, Mucedola, Italy) and tap water were available ad libitum before and immediately after the drug administration.

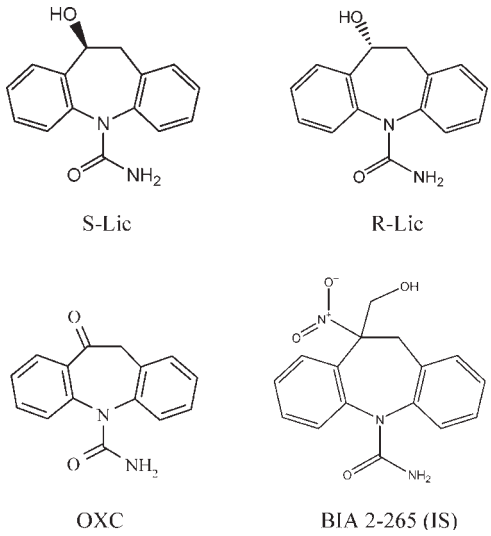

Fig. 1. Chemical structures of *S*-licarbazepine (*S*-Lic), *R*-licarbazepine (*R*-Lic), oxcarbazepine (OXC) and BIA 2-265 used as internal standard (IS).

S-Lic and *R*-Lic were suspended in a 0.5% carboxymethylcellulose aqueous solution. Groups of eight mice per time point received a single dose of *S*-Lic or *R*-Lic (350 mg/kg) by oral gavage (0.5 ml/30 g mouse weight). Blood samples, brain, liver and kidney tissues were taken at 0.25, 0.5, 0.75, 1, 2, 4, 6, 10, 16 and 24 h post-dose. Blood samples were collected into heparinized tubes by decapitation preceded of cervical dislocation. The plasma was separated by centrifugation at 4000 rpm for 10 min (4°C) and stored at −30°C until analysis. After exsanguination, brain, liver, and kidneys were quickly removed, weighed and then homogenized (4 ml/g) in a 0.1M sodium phosphate buffer (pH 5). The tissue homogenates were centrifuged at 4800 rpm for 15 min (4°C) and the supernatants were also stored at −30°C until analysis.

All animal experimentation was conducted in accordance with the European Directive (86/609/EEC) for the accommodation and care of laboratory animals and the experimental procedures were approved by the Portuguese Veterinary General Division.

Determination of Licarbazepine Enantiomers and OXC

Plasma and tissue concentrations of *S*-Lic, *R*-Lic and OXC were determined by an enantioselective HPLC-UV-SPE assay previously developed and validated.[21] Briefly, an aliquot of each plasma sample (250 μl) was added to 750 μl of 0.1M sodium phosphate buffer (pH 5) spiked with 2 μg of the IS. The samples were vortex-mixed and loaded into Waters Oasis® HLB extraction cartridges (30 mg, 1 ml; Milford, MA), which were previously condi-

tioned with 1 ml of methanol, 1 ml of acetonitrile and 1 ml of water/acetonitrile (95:5, v/v). After sample elution, the loaded cartridges were submitted to −30 kPa and washed twice with 1 ml of water and twice with 1 ml of water/acetonitrile (95:5, v/v). After drying the sorbent under airflow for 5 min, the drugs were eluted with 1 ml of ethyl acetate under a gentle vacuum and then the cartridges were dried for 30 sec at −30 kPa. The eluates were evaporated to dryness under a nitrogen stream at 45°C and the residues reconstituted in 100 μl of water/methanol (88:12, v/v), vortexed for ∼30 sec and placed in an ultrasonic bath at room temperature for ∼1 min. Following this, the reconstituted extracts were transferred to 0.22 μm Spin-X centrifugal filters, centrifuged at 13,400 rpm for 2 min and 20 μl of the final filtered extract were used for HPLC analysis. The supernatants of brain, liver and kidney homogenates were centrifuged (13,400 rpm for 20 min) a second time to give clear supernatants of which 1 ml (∼250 μg of tissue) was also spiked with 2 μg of the IS. Next the drugs in the brain, liver, and kidney supernatants were extracted by the solid-phase extraction procedure already described for plasma samples, with some differences in the washing steps and vacuum conditions (−40 kPa). As tissue matrices are more complex than plasma, the loaded cartridges were washed with 1 ml of water and 1 ml of water/acetonitrile (95:5, v/v) three and four times in brain samples and in liver/kidney samples, respectively.

The HPLC analysis was performed on a BAS-480 Liquid Chromatograph equipped with a PM-80 pump, a Rheodyne manual injector with a 20-μl loop, a BAS UV-116 UV-Vis detector, a BAS LC-22C Temperature Controller, a BAS DA-5 Chromatography Control and a Data System Interface (all from Bioanalytical Systems, West Lafayette, IN). Data collection and integration were achieved by means of a BAS Chromgraph Control and Chromgraph Report software version 2.30. The chromatographic separation was carried out at 30°C by isocratic elution with water/methanol (88:12, v/v), at a flow rate of 0.7 ml/min, on a LiChroCART 250-4 ChiraDex (β-cyclodextrin, 5 μm) column protected by a LiChroCART 4-4 ChiraDex (β-cyclodextrin, 5 μm) guard column purchased from Merck KGaA (Darmstadt, Germany). The detector was set at 225 nm. The method was linear for OXC over concentration ranges 0.4–8 μg/ml in mouse plasma, 0.1–1.5 μg/ml in supernatant of brain homogenate and 0.1–2 μg/ml in supernatant of liver/kidney homogenates, and for each licarbazepine enantiomer in the ranges of 0.4–80 μg/ml, 0.1–15 μg/ml and 0.1–20 μg/ml in plasma, brain, and liver/kidney, respectively. The precision and accuracy were lower than 15%. No peaks due to the plasma and tissues interfered at the retention time of the analytes. The limit of quantification (LOQ) was 0.4 μg/ml in plasma and 0.1 μg/ml (∼0.4 μg/g) in supernatants of tissue homogenates.

Pharmacokinetic Analysis

The peak concentration of *S*-Lic, *R*-Lic and OXC in plasma and tissues (C_{max}) and the time to reach C_{max} (t_{max}) were obtained directly from the experimental data. Other pharmacokinetic parameters were computed from the mean concentration data ($n = 8$) obtained at each time point by non-compartmental analysis using the WinNonlin® Version 4.1 (Pharsight, Mountain View, CA): area under the concentration-time curve (AUC) from time zero to the last sampling time at which concentrations were at or above the LOQ (AUC_{0-t}), calculated by the linear trapezoidal rule; AUC from time zero to infinite ($AUC_{0-\infty}$), calculated from $AUC_{0-t} + (C_{last}/\lambda_z)$, where C_{last} is the last quantifiable concentration and λ_z is the apparent terminal rate constant calculated by log-linear regression of the terminal segment of the concentration–time profile; apparent terminal elimination half-life ($t_{1/2}$) and mean residence time (MRT). Mean plasma and tissue concentrations lower than the LOQ of the assay were taken as zero for all calculations.

RESULTS

Plasma and Brain, Liver and Kidney Tissue Disposition of S-*Lic*

The mean plasma and brain, liver and kidney tissue concentration–time profiles of *S*-Lic and their metabolites (OXC and *R*-Lic), following oral administration of pure *S*-Lic enantiomer at 350 mg/kg to mice, are presented in Figure 2. The corresponding pharmacokinetic parameters estimated by non-compartmental analysis are summarized in Table 1. The peak concentrations of *S*-Lic were reached at the earliest sampling time point (0.25 h) in plasma, liver and kidneys, demonstrating that the parent drug is rapidly absorbed. As expected, the peak brain concentration of *S*-Lic was attained later (2 h) than in plasma. Figure 2 shows that in mice *S*-Lic is metabolized to a small extent with OXC and *R*-Lic being its major and minor metabolites, respectively. Indeed, following its own administration, *S*-Lic corresponded to approximately 85, 77, 90 and 92% of total drug exposure in plasma, brain, liver and kidneys, respectively (as assessed by $AUC_{0-\infty}$). In the same way, the metabolite OXC represented ∼15, 23, 10, and 8% in the corresponding matrices. The drug exposure to *R*-Lic was substantially lower representing less than 0.24% in liver, whereas in kidney tissue it was found in measurable amounts just at 0.25-h post-dose, not allowing the calculation of the corresponding $AUC_{0-\infty}$.

To assess the rate and the extent of tissue distribution of *S*-Lic and its metabolites, the corresponding C_{max} and $AUC_{0-\infty}$ tissue/plasma ratios were calculated for brain, liver and kidneys, and are displayed in the Table 2. First of all, the C_{max} and $AUC_{0-\infty}$ tissue/plasma ratios were not available for *R*-Lic, because its plasma levels were found below the LOQ of the analytical method. All estimated values for brain/plasma ratios were lower than the unity, demonstrating higher plasma drug concentrations. These data also indicated that the distribution of *S*-Lic into the brain was less favorable than that for OXC. In fact, the rate and the extension of OXC brain penetration were, respectively, 2.1 and 1.7 times greater than those for *S*-Lic. Moreover, as shown in the Table 1, the t_{max} of *S*-Lic in the brain was quite displaced to the right comparatively to that in plasma, whereas for OXC the t_{max} in brain and in plasma were coincident. On the other hand, in agreement with

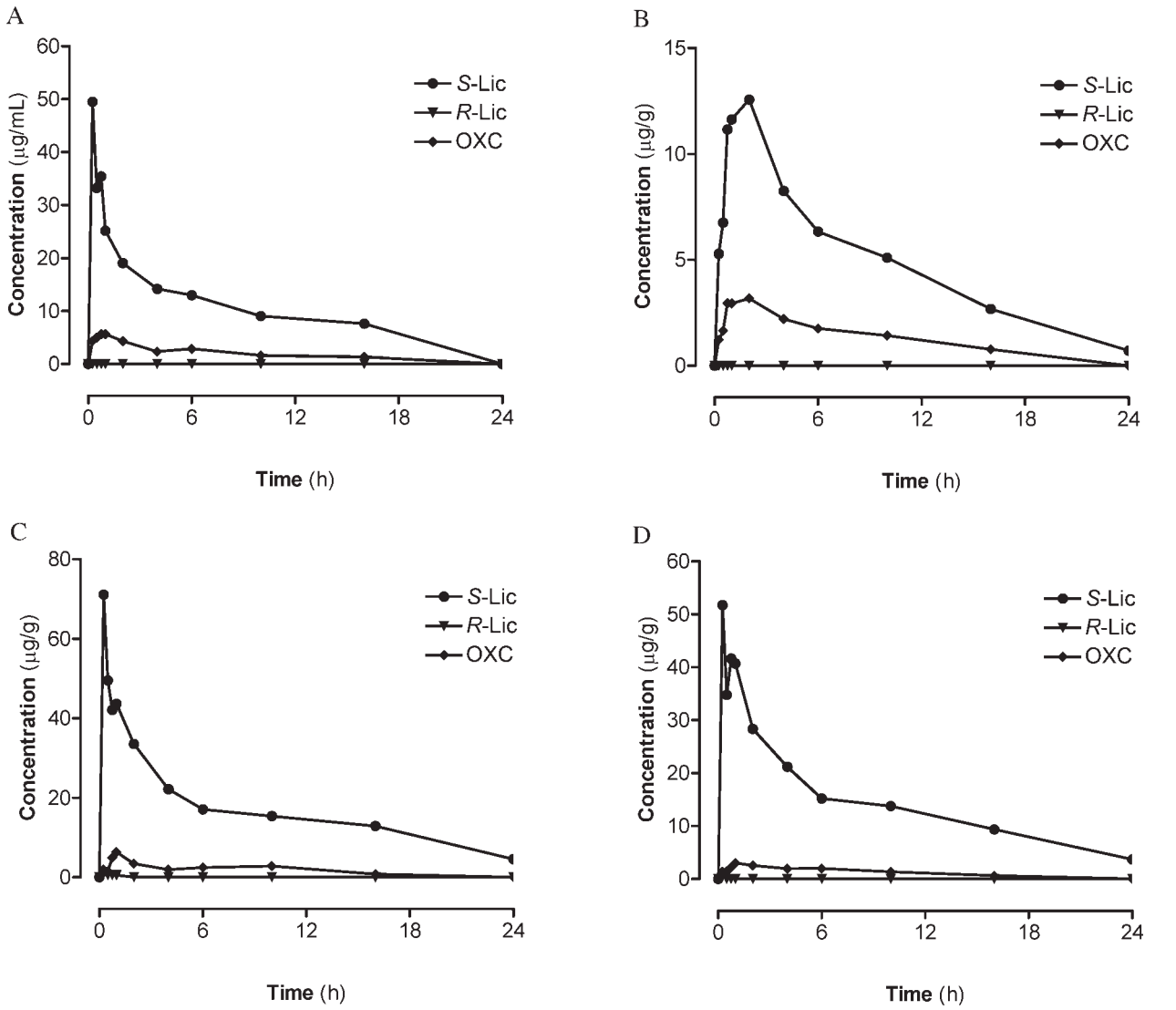

Fig. 2. Mean plasma (**A**), brain (**B**), liver (**C**), and kidney (**D**) concentration–time profiles of *S*-Lic, *R*-Lic, and OXC following a single oral administration of *S*-Lic 350 mg/kg to mice. Symbols represent the means of eight mice.

the values of C_{max} and $AUC_{0-\infty}$ liver and kidney/plasma ratios, the predisposition for liver and kidney storage of *S*-Lic is evident in contrast to OXC, which appeared to in a larger extent in plasma. However, the C_{max} and $AUC_{0-\infty}$ liver/plasma ratios for *S*-Lic were shown to be greater than those in kidneys, supporting that the liver will be its main deposit.

Regarding the $t_{1/2}$ and MRT parameters of all compounds in all matrices (Table 1), an aspect that deserves to be pointed out is the very low $t_{1/2}$ and MRT values estimated for *R*-Lic in liver.

Plasma and Brain, Liver and Kidney Tissue Disposition of R-*Lic*

The mean plasma and brain, liver and kidney tissue concentration–time profiles of *R*-Lic and its metabolites (OXC and *S*-Lic) were also determined in mice after a single oral dose of *R*-Lic enantiomer at 350 mg/kg (see Fig. 3). However, it is important to stress that in addition to OXC and *S*-Lic, another more polar metabolite was detected in considerable amounts, which was not quantified because the method was not validated for that purpose. Consequently, when possible, plasma and tissue pharmacokinetic parameters of *R*-Lic, *S*-Lic, and OXC were calculated by non-compartmental model and the most relevant parameters are summarized in Table 3. Taking into account the data presented, it is evident that the highest plasma, liver and kidney *R*-Lic concentrations were achieved at first sampling time point (0.25 h) and, at that moment, its brain levels were already elevated and close to the maximal brain concentration (Figure 3B). Hence, these findings showed that *R*-Lic is rapidly absorbed from the mouse gastrointestinal tract and is quickly distributed. Undoubtedly, following its oral administration to mice, *R*-Lic was found to be the major compound in plasma and in all assayed tissues over the full sampling time range. OXC and *S*-Lic were

TABLE 1. Plasma, brain, liver, and kidney pharmacokinetic parameters of *S*-Lic and its metabolites *R*-Lic and OXC in mice after a single oral dose of *S*-Lic 350 mg/kg

Pharmacokinetic parameters	*S*-Lic	*R*-Lic	OXC
Plasma			
t_{max} (h)	0.25	NA	0.75
C_{max} (μg/mL)	49.47	NA	5.65
AUC_{0-t} (μg h/mL)	209.18	NC	39.08
$AUC_{0-\infty}$ (μg h/mL)	310.49	NC	53.10
$t_{1/2}$ (h)	9.25	NC	7.22
MRT (h)	13.60	NC	11.37
Brain			
t_{max} (h)	2.00	NA	0.75
C_{max} (μg/g)	12.56	NA	2.95
AUC_{0-t} (μg h/g)	114.46	NC	27.20
$AUC_{0-\infty}$ (μg h/g)	120.41	NC	35.47
$t_{1/2}$ (h)	5.74	NC	7.40
MRT (h)	8.67	NC	11.01
Liver			
t_{max} (h)	0.25	0.25	1.00
C_{max} (μg/g)	71.13	0.87	6.38
AUC_{0-t} (μg h/g)	399.55	0.95	39.08
$AUC_{0-\infty}$ (μg h/g)	446.40	1.16	47.16
$t_{1/2}$ (h)	7.18	0.82	6.87
MRT (h)	10.96	1.24	9.87
Kidney			
t_{max} (h)	0.25	0.25	1.00
C_{max} (μg/g)	51.71	0.55	3.01
AUC_{0-t} (μg h/g)	336.89	NC	25.42
$AUC_{0-\infty}$ (μg h/g)	375.37	NC	31.79
$t_{1/2}$ (h)	7.26	NC	7.08
MRT (h)	10.62	NC	10.26

C_{max} and t_{max} are experimental values; AUC_{0-t}, $AUC_{0-\infty}$, $t_{1/2}$, and MRT values were calculated by non-compartmental analysis from mean concentrations at each time point (n = 8 mice per group). NA, not available; NC, not calculated.

produced to a small extent possibly by *R*-Lic oxidation and isomerization, respectively. *S*-Lic concentrations were found above the LOQ of the assay in plasma, liver and kidneys, while OXC was quantified in all matrices.

Once again, to evaluate the rate and the extent of tissue distribution of *R*-Lic and its metabolites, the corresponding C_{max} and $AUC_{0-\infty}$ tissue/plasma ratios were estimated for brain, liver and kidneys (Table 4). The C_{max} and $AUC_{0-\infty}$ brain/plasma ratios for *R*-Lic and OXC were far lower than the unity, which support their poor penetration into the brain. However, in spite of the extent of brain distribution is similar for both *R*-Lic and OXC (as assessed by $AUC_{0-\infty}$), the value of the C_{max} brain/plasma ratio was 3.6 times higher for OXC, suggesting some differences in their blood–brain barrier (BBB) crossing rate. Actually, as shown in the Table 3, the t_{max} of *R*-Lic was observed former in plasma than in brain, whereas the t_{max} of OXC was synchronized in both matrices, indicating that OXC crosses the BBB more promptly than *R*-Lic. In this case, as *S*-Lic brain concentrations were lower than the LOQ of the assay, the corresponding C_{max} and $AUC_{0-\infty}$ brain/plasma ratios could not be calculated. Taking into consideration the C_{max} and $AUC_{0-\infty}$ liver/plasma ratios for the parent compound (*R*-Lic), its lack of ability for accumulation (ratios near the unity) is evident. In contrast, the *S*-Lic formed as a metabolite of *R*-Lic trends towards hepatic accumulation and the metabolite OXC undergoes hepatic release into the systemic circulation. Likewise, the kidney/plasma ratios support the renal storage of *S*-Lic produced but to a lesser degree than that occurring in liver. Finally, *R*-Lic and OXC appeared in greater amounts in plasma than in kidneys.

Stereoselective Distribution of S-Lic and R-Lic

The differential distribution of *S*-Lic and *R*-Lic enantiomers in plasma and brain, liver and kidney tissues, following their separate administration to mice, was studied based on their stereoselective index (enantiomeric ratio),[22] of the mean values of C_{max} and $AUC_{0-\infty}$ pharmacokinetic parameters. Levy and Boddy[22] considered a measurable difference in the parameter values for a pair of enantiomers when it is greater than or equal to 20%. In mice treated with 350 mg/kg of *S*-Lic or *R*-Lic by oral gavage, remarkable differences in the disposition of licarbazepine enantiomers were recorded (see Figure 4). The $AUC_{0-\infty}$ S/R ratios were higher than the unity in all matrices, indicating a greater exposure to *S*-Lic than *R*-Lic after equivalent dosing regime. In fact, the systemic exposure to *S*-Lic and *R*-Lic was comparable, but even so large differences in their brain, liver and kidney exposure were identified. Indeed these data support the hepatic and renal uptake of S-enantiomer as well as its larger distribution (almost twice) to the brain, demonstrating the chiral discrimination of *S*-Lic and *R*-Lic in a living system. Moreover, the corresponding C_{max} S/R ratios of 0.66 in plasma and 0.95 in liver and kidneys, observed at 0.25 h postdose, confirm an increased affinity of *S*-Lic to liver and kidney tissues from the earliest time points.

Stereoselective Metabolism of S-*Lic and* R-*Lic and Chiral Inversion*

Undoubtedly, analyzing the mean plasma and brain, liver and kidney tissue concentration–time profiles obtained after the administration of *S*-Lic and *R*-Lic to mice (Figures 2 and 3), it is obvious that each parent compound was the main responsible for the systemic or tissue drug exposure. It is also evident that OXC is a common metabolite produced either from *S*-Lic or *R*-Lic, which appeared in measurable amounts in all matrices. Thus, in order to compare the formation of OXC from both enantiomers, the corresponding C_{max} and $AUC_{0-\infty}$ ratios were calculated and

TABLE 2. Brain, liver, and kidney/plasma $AUC_{0-\infty}$ and C_{max} ratios of *S*-Lic, *R*-Lic, and OXC obtained after oral administration of *S*-Lic (350 mg/kg) by oral gavage to mice

	C_{max}			$AUC_{0-\infty}$		
Ratio	*S*-Lic	*R*-Lic	OXC	*S*-Lic	*R*-Lic	OXC
Brain/plasma	0.25	NA	0.52	0.39	NA	0.67
Liver/plasma	1.44	NA	1.13	1.44	NA	0.89
Kidney/plasma	1.05	NA	0.53	1.21	NA	0.60

NA, not available.

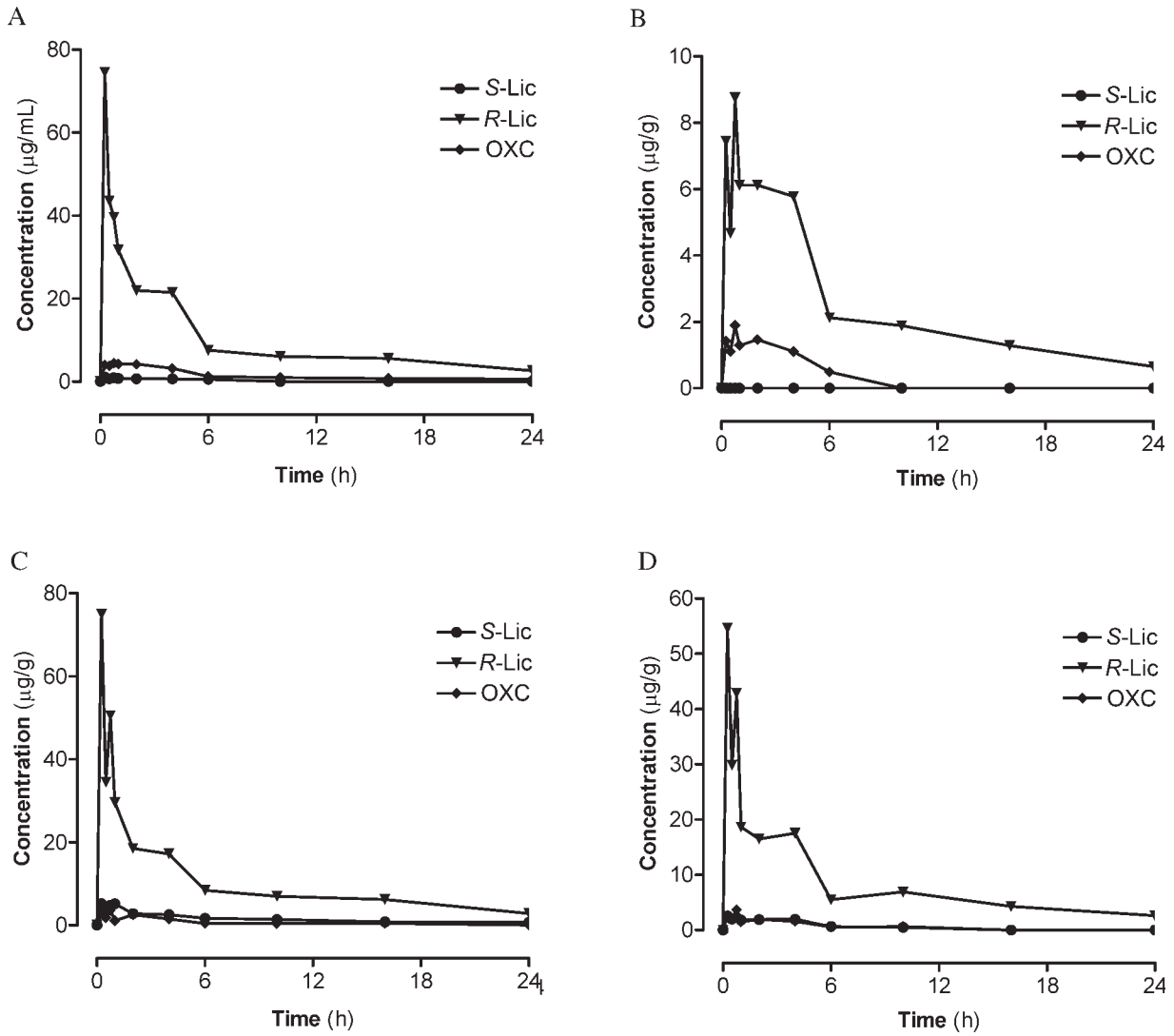

Fig. 3. Mean plasma (**A**), brain (**B**), liver (**C**), and kidney (**D**) concentration–time profiles of *R*-Lic, *S*-Lic, and OXC following a single oral administration of *R*-Lic 350 mg/kg to mice. Symbols represent the means of eight mice.

are represented in Figure 5. These data clearly support that *S*-Lic was metabolized to OXC to a greater extent than *R*-Lic. At this point it should be pointed out that the brain exposure to OXC is approximately four times higher after *S*-Lic administration. Finally, the occurrence of enantiomeric inversion of *S*-Lic and *R*-Lic in mice should be reported. By treatment with *S*-Lic, some amounts of *R*-Lic were produced and following *R*-Lic administration its antipode was also formed (Tables 1 and 3). Taking into account the pharmacokinetic profiles obtained, a strict parallel was observed between the parent compounds and their opposite enantiomer (Figures 2 and 3). Hence, these findings suggest the ability of the mouse to perform the interconversion of both licarbazepine enantiomers, albeit to a small extent. To identify the preferential direction of enantiomeric bioinversion, when possible, the C_{max} and $AUC_{0-\infty}$ pharmacokinetic parameters of *S*-Lic and *R*-Lic produced by administration of their complementary enantiomer were compared (Table 5). As indicated, the production of *S*-Lic from *R*-Lic was much more favorable. In fact, the hepatic exposure to *S*-Lic after *R*-Lic administration was approximately 40 times greater than that observed for *R*-Lic following *S*-Lic administration (as assessed by $AUC_{0-\infty}$). Finally, the stereoselectivity in the metabolism of licarbazepine enantiomers was also supported by the formation of an additional metabolite from *R*-Lic.

DISCUSSION

The interest in three-dimensional molecular structure of drugs was largely ignored during decades of pharmaceutical research, but recently, it has emerged as a key issue in drug design, discovery, development and regulatory fields.[5] In fact, chirality is one of the main features of living systems and the interactions of drugs with corresponding biological targets may be stereoselective.[1,2] Therefore, at the present time, the majority of the new drugs reaching

TABLE 3. Plasma, brain, liver, and kidney pharmacokinetic parameters of *R*-Lic and its metabolites *S*-Lic and OXC in mice after a single oral dose of *R*-Lic 350 mg/kg

Pharmacokinetic parameters	*R*-Lic	*S*-Lic	OXC
Plasma			
t_{max} (h)	0.25	0.25	0.75
C_{max} (μg/mL)	74.55	1.09	4.43
AUC_{0-t} (μg h/mL)	237.22	4.16	34.69
$AUC_{0-\infty}$ (μg h/mL)	282.68	11.67	42.21
$t_{1/2}$ (h)	12.24	8.98	8.47
MRT (h)	12.30	13.21	12.54
Brain			
t_{max} (h)	0.75	NA	0.75
C_{max} (μg/g)	8.76	NA	1.89
AUC_{0-t} (μg h/g)	57.21	NC	6.81
$AUC_{0-\infty}$ (μg h/g)	64.38	NC	9.10
$t_{1/2}$ (h)	7.63	NC	3.25
MRT (h)	10.27	NC	4.62
Liver			
t_{max} (h)	0.25	0.25	0.75
C_{max} (μg/g)	74.96	5.24	3.59
AUC_{0-t} (μg h/g)	235.88	36.76	14.05
$AUC_{0-\infty}$ (μg h/g)	263.44	46.25	18.04
$t_{1/2}$ (h)	6.74	9.06	6.14
MRT (h)	9.98	14.03	9.38
Kidney			
t_{max} (h)	0.25	0.25	0.75
C_{max} (μg/g)	54.62	2.52	3.66
AUC_{0-t} (μg h/g)	194.11	12.52	12.05
$AUC_{0-\infty}$ (μg h/g)	227.96	15.43	16.28
$t_{1/2}$ (h)	9.18	4.16	4.56
MRT (h)	11.59	5.92	6.99

C_{max} and t_{max} are experimental values; AUC_{0-t}, $AUC_{0-\infty}$, $t_{1/2}$ and MRT values were calculated by non-compartmental analysis from mean concentrations at each time point (n = 8 mice per group); NA, not available; NC, not calculated.

the market are single enantiomers rather than racemic mixtures to improve the therapeutic index, given that one of the enantiomers may be inactive or even counterproductive to the therapeutic effect.[2,4]

It is widely accepted that the stereochemistry has little influence on passive processes such as diffusion across membranes. However, when the drug interacts with an enzyme or a transporter system the chiral discrimination may be seen, at least, if the drug stereogenic center(s) are important in its target interaction.[23] Metabolism has been shown to be the most important pharmacokinetic process

TABLE 4. Brain, liver, and kidney/plasma $AUC_{0-\infty}$ and C_{max} ratios of *R*-Lic, *S*-Lic and OXC obtained after oral administration of *R*-Lic (350 mg/kg) by oral gavage to mice

	C_{max}			$AUC_{0-\infty}$		
Ratio	*R*-Lic	*S*-Lic	OXC	*R*-Lic	*S*-Lic	OXC
Brain/plasma	0.12	NA	0.43	0.23	NA	0.22
Liver/plasma	1.01	4.81	0.81	0.93	3.96	0.43
Kidney/plasma	0.73	2.31	0.83	0.81	1.32	0.39

NA, not available.

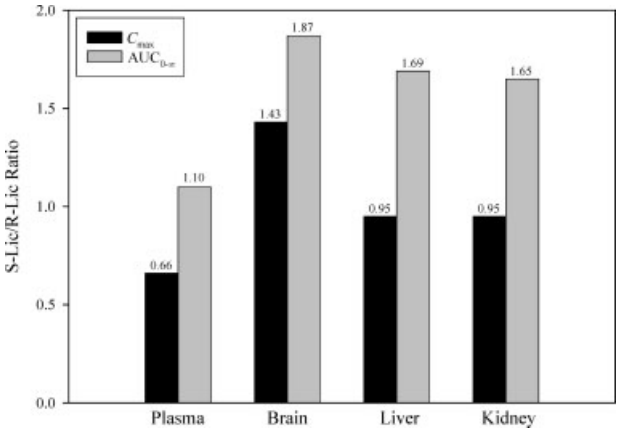

Fig. 4. The C_{max} and $AUC_{0-\infty}$ S/R enantiomeric ratios of *S*-Lic and *R*-Lic in plasma and brain, liver and kidney tissues after their separate administration (350 mg/kg) to mice by oral gavage.

in enantioselective drug disposition, but plasma and tissue protein binding as well as membrane permeability may also play a preponderant role.[24] Thereby, the liver and kidney pharmacokinetic behavior of *S*-Lic and *R*-Lic enantiomers and their brain uptake were investigated in mice. These biological matrices were chosen, firstly, because the brain is the therapeutic target of licarbazepine enantiomers, and secondly, the liver and kidneys are the most important organs from a pharmacokinetic point of view, being respectively, the primary organ for drug metabolism and drug excretion. In the present study, *S*-Lic and *R*-Lic plasma protein binding were not determined due to their low binding percentage (<30%) in dogs, which was almost identical for both enantiomers.[20] In humans, the licarbazepine plasma protein binding was found to be ~40%.[12,15]

Our results demonstrated that *S*-Lic and *R*-Lic are rapidly absorbed from the mouse gastrointestinal tract and rapidly distributed after their own administration, at least for the highly perfused tissues. From the overall data obtained, the enantioselectivity in licarbazepine absorption appears to be unlikely, because the liver concentrations of

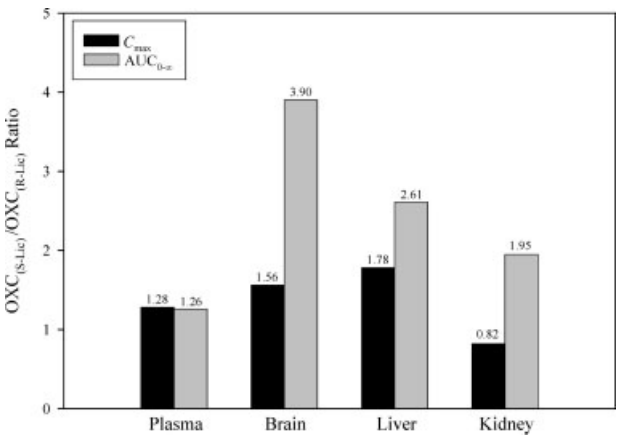

Fig. 5. The C_{max} and $AUC_{0-\infty}$ OXC ratios in plasma and brain, liver and kidney tissues after separate administration of *S*-Lic and *R*-Lic (350 mg/kg) to mice by oral gavage.

TABLE 5. Enantiomeric interconversion of *S*-Lic and *R*-Lic after their separate administration to mice by oral gavage (350 mg/kg)

	$S\text{-Lic}_{(R\text{-Lic})}/R\text{-Lic}_{(S\text{-Lic})}$	
Ratio	C_{max}	$AUC_{0-\infty}$
Plasma	NA	NA
Brain	NA	NA
Liver	6.02	39.9
Kidney	4.58	NA

$S\text{-Lic}_{(R\text{-Lic})}$, *S*-Lic produced from *R*-Lic; $R\text{-Lic}_{(S\text{-Lic})}$, *R*-Lic produced from S-Lic; NA, not available.

both enantiomers after their separate administration are similar at first sampling time point (0.25 h). However, at that time, the value of the stereoselective index (1.51) between *R*-Lic and *S*-Lic plasma concentrations already reflect their stereoselective first-pass effect. It was demonstrated that *S*-Lic undergoes hepatic and renal accumulation either after its own administration or when formed as a metabolite of *R*-Lic. Hence, liver and kidneys act like reservoirs of *S*-Lic. From the metabolic data, it is also evident that OXC was produced from both licarbazepine enantiomers, being generated to a higher extent from *S*-Lic. However, less obvious may be the source of the small amounts of *S*-Lic and *R*-Lic produced following the administration of the corresponding antipode. At this moment, it is important to consider that the reduction of OXC not occurs effectively in mice, in contrast to man.[9] Moreover, the t_{max} values were coincident for both administered and produced licarbazepine enantiomers, whereas the t_{max} for OXC occurred later. Consequently, the bi-directional chiral inversion of licarbazepine enantiomers occurred in mice probably through a liver racemase, which favors the production of *S*-Lic from *R*-Lic, and not through OXC reduction. In fact, the chiral inversion is always mediated by enzymes and, in humans, was firstly demonstrated with ibuprofen.[25] The extra metabolite produced in mice after treatment with *R*-Lic, most likely, will correspond to the *trans*-diol. These results are in agreement with the observations performed by Hainzl et al.[9] demonstrating that the *trans*-diol is only produced from *R*-Lic. The formation of the *trans*-diol will probably contribute to an earlier inactivation of *R*-Lic. After all, taking into consideration the data presented and the information provided by Hainzl et al.,[9] the proposed metabolic pathways for *S*-Lic and *R*-Lic in mice are represented in Figure 6.

From this work, another relevant part of data was the stereoselective brain disposition of *S*- and *R*-Lic enantiomers. To our knowledge, these findings are reported here for the first time. Although their comparable systemic exposure ($AUC_{0-\infty}$ S/R plasma ratio close to unity), the extent of brain penetration for *S*-Lic was found to be approximately 2 times greater than that for *R*-Lic. Indeed, as other central nervous system drugs, *S*-Lic and *R*-Lic must overcome the BBB to reach the brain parenchyma, with their brain concentrations being much lower than those in plasma. Actually, the BBB consists of various transporter proteins involved in the active influx and efflux of drugs to and from the brain.[26] Thus, as with other drugs, licarbazepine enantiomers may be substrates for multidrug transporters (MDT) including *P*-glycoprotein at the BBB,[27] being subject to efflux transport and, possibly, *R*-Lic will be the preferential substrate. Previously, Clinckers et al.[28] demonstrated that OXC is a substrate for MDT at the BBB, which actively limits the penetration and accumulation of OXC into the brain.

In 1991, Levy and Boddy[22] considered three distinct organizational levels in the body (macromolecular, whole-organ and whole-body) and suggested that degree of stereoselectivity is more pronounced and easier to detect in front of macromolecular-specific or organ-specific parameters than in whole-body pharmacokinetic parameters. Indeed, our data appear to reflect this general theory: first of all an additional metabolite was formed from *R*-Lic, detecting stereoselectivity in the presence of metabolic enzymes; secondly, considering the $AUC_{0-\infty}$ pharmacokinetic parameter, the stereoselectivity between *S*- and *R*-Lic was greater in whole-organ level (brain, liver, and kidney) than in whole-body (see Fig. 4).

Despite the obvious species differences between mouse and man, these data give new information related to the pharmacokinetic disposition of licarbazepine enantiomers and their ability to cross the BBB and attain their therapeutic target. At last, the stereoselectivity identified in the disposition of *S*-Lic and *R*-Lic may also explain the differences observed in the systemic drug exposure to ESL and OXC. Indeed, Bialer et al.[29] reported that the bioavailability of ESL, measured in terms of *S*-Lic and *R*-Lic AUC, was 16% greater than that for OXC after intake of an equivalent molar dose.

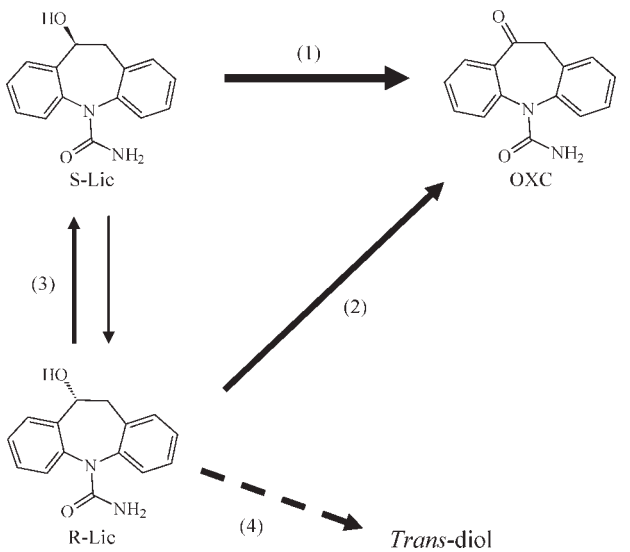

Fig. 6. Proposed metabolism of *S*-Lic and *R*-Lic in mice. The thickness of the arrows indicates the relative extent of the metabolic pathways: OXC is the major metabolite of *S*-Lic (1) and *R*-Lic (2), enantiomeric inversion is favorable to the formation of *S*-Lic (3) and conjugating the data of this study with the findings reported by Hainzl et al.[9] the *trans*-diol metabolite is produced only from *R*-Lic (4).

LITERATURE CITED

1. Andersson T. Single-isomer drugs: true therapeutic advances. Clin Pharmacokinet 2004;43:279–285.
2. Kan AY, Preskorn SH, Wimalasena K. Single enantiomer drugs: should they be developed? Essent Psychopharmacol 2006;7:15–23.
3. Hutt AJ, Tan SC. Drug chirality and its clinical significance. Drugs 1996;52 (Suppl 5):1–12.
4. Agranat I, Caner H, Caldwell J. Putting chirality to work: the strategy of chiral switches. Nat Rev Drug Discov 2002;1:753–768.
5. Hutt AJ. The development of single-isomer molecules: why and how. CNS Spectr 2002;7 (Suppl 1):14–22.
6. Agrawal YK, Bhatt HG, Raval HG, Oza PM, Gogoi PJ. Chirality—a new era of therapeutics. Mini Rev Med Chem 2007;7:451–460.
7. Elger C, Bialer M, Cramer JA, Maia J, Almeida L, Soares-da-Silva P. Eslicarbazepine acetate: a double-blind, add-on, placebo-controlled exploratory trial in adult patients with partial-onset seizures. Epilepsia 2007;48:497–504.
8. Benes J, Parada A, Figueiredo AA, Alves PC, Freitas AP, Learmonth DA, Cunha RA, Garrett J, Soares-da-Silva P. Anticonvulsant and sodium channel-blocking properties of novel 10,11-dihydro-5H-dibenz[b,f] azepine-5-carboxamide derivatives. J Med Chem 1999;42:2582–2587.
9. Hainzl D, Parada A, Soares-da-Silva P. Metabolism of two new antiepileptic drugs and their principal metabolites S(+)- and R(−)-10,11-dihydro-10-hydroxy carbamazepine. Epilepsy Res 2001;44:197–206.
10. Matar KM, Nicholls PJ, Bawazir SA, Al-Hassan MI, Tekle A. Effect of valproic acid on the pharmacokinetic profile of oxcarbazepine in the rat. Pharm Acta Helv 1999;73:247–250.
11. Bialer M. New antiepileptic drugs that are second generation to existing antiepileptic drugs. Expert Opin Investig Drugs 2006;15:637–647.
12. May TW, Korn-Merker E, Rambeck B. Clinical pharmacokinetics of oxcarbazepine. Clin Pharmacokinet 2003;42:1023–1042.
13. Flesch G, Francotte E, Hell F, Degen PH. Determination of the R-(−) and S-(+) enantiomers of the monohydroxylated metabolite of oxcarbazepine in human plasma by enantioselective high-performance liquid chromatography. J Chromatogr 1992;581:147–151.
14. Volosov A, Xiaodong S, Perucca E, Yagen B, Sintov A, Bialer M. Enantioselective pharmacokinetics of 10-hydroxycarbazepine after oral administration of oxcarbazepine to healthy Chinese subjects. Clin Pharmacol Ther 1999;66:547–553.
15. Flesch G. Overview of the clinical pharmacokinetics of oxcarbazepine. Clin Drug Investig 2004;24:185–203.
16. Bialer M, Johannessen SI, Kupferberg HJ, Levy RH, Perucca E, Tomson T. Progress report on new antiepileptic drugs: a summary of the Eighth Eilat Conference (EILAT VIII). Epilepsy Res 2007;73:1–52.
17. Almeida L, Soares-da-Silva P. Safety, tolerability and pharmacokinetic profile of BIA 2-093, a novel putative antiepileptic agent, during first administration to humans. Drugs R D 2003;4:269–284.
18. Almeida L, Soares-da-Silva P. Safety, tolerability, and pharmacokinetic profile of BIA 2-093, a novel putative antiepileptic, in a rising multiple-dose study in young healthy humans. J Clin Pharmacol 2004;44:906–918.
19. Almeida L, Falcão A, Maia J, Mazur D, Gellert M, Soares-da-Silva P. Single-dose and steady-state pharmacokinetics of eslicarbazepine acetate (BIA 2-093) in healthy elderly and young subjects. J Clin Pharmacol 2005;45:1062–1066.
20. Volosov A, Yagen B, Bialer M. Comparative stereoselective pharmacokinetic analysis of 10-hydroxycarbazepine after oral administration of its individual enantiomers and the racemic mixture to dogs. Epilepsia 2000;41:1107–1111.
21. Alves G, Figueiredo I, Castel-Branco M, Loureiro A, Falcão A, Caramona M. Simultaneous and enantioselective liquid chromatographic determination of eslicarbazepine acetate, *S*-licarbazepine, *R*-licarbazepine and oxcarbazepine in mouse tissue samples using ultraviolet detection. Anal Chim Acta 2007;596:132–140.
22. Levy RH, Boddy AV. Stereoselectivity in pharmacokinetics: a general theory. Pharm Res 1991;8:551–556.
23. Caldwell J. Importance of stereospecific bioanalytical monitoring in drug development. J Chomatogr A 1996;719:3–13.
24. Rentsch KM. The importance of stereoselective determination of drugs in clinical laboratory. J Biochem Biophys Methods 2002;54:1–9.
25. Wsól V, Skálová L, Szotáková B. Chiral inversion of drugs: coincidence or principle? Curr Drug Metab 2004;5:517–533.
26. Gupta A, Chatelain P, Massingham R, Jonsson EN, Hammarlund-Udenaes M. Brain distribution of cetirizine enantiomers: comparison of three different tissue-to-plasma partition coefficients: K_p, $K_{p,u}$, and $K_{p,uu}$. Drug Metab Dispos 2006;34:318–323.
27. Doan KMM, Humphreys JE, Webster LO, Wring SA, Shampine LJ, Serabjit-Singh CJ, Adkison KK, Polli JW. Passive permeability and *P*-glycoprotein-mediated efflux differentiate central nervous system (CNS) and non-CNS marketed drugs. J Pharmacol Exp Ther 2002;303:1029–1037.
28. Clinckers R, Smolders I, Meurs A, Ebinger G, Michotte Y. Quantitative in vivo microdialysis study on the influence of multidrug transporters on the blood–brain barrier passage of oxcarbazepine: concomitant use of hippocampal monoamines as pharmacodynamic markers for the anticonvulsant activity. J Pharmacol Exp Ther 2005;314:725–731.
29. Bialer M, Johannessen SI, Kupferberg HJ, Levy RH, Perucca E, Tomson T. Progress report on new antiepileptic drugs: a summary of the Seventh Eilat Conference (EILAT VII). Epilepsy Res 2004;61:1–48.